Texture-Related Roughness of (Nb,Ti)N Sputter-Deposited Films

N. N. Iosad, N. M. van der Pers, S. Grachev, M. Zuiddam, B. D. Jackson, P. N. Dmitriev, and T. M. Klapwijk

Abstract—We study the properties of (Nb,Ti)N films deposited by reactive magnetron sputtering in an atmosphere of argon and nitrogen at ambient substrate temperature, focusing, in particular, on the technological factors determining film texture and roughness. We find that increasing the adatom energy, while keeping the film chemical composition constant, results in a change of texture from [111] to [100]. Similar changes in film texture are observed as the nitrogen injection decreases for a constant sputtering pressure, indicating that adatom energy is not the only one determining factor. Analyzing the experimental data, it is concluded that nitrogen concentration has a very strong influence on the process of the texture formation, since an increase in nitrogen injection results in an increase in adatom energy, while the film growth is driven toward [111] texturing. Film roughness is strongly related with texture in both experiments, i.e., decreases with an increase in the ratio of [200] and [111] XRD line intensities, indicating that film roughness is determined by crystal habit.

Index Terms—Coatings, magnetron sputtering, superconducting devices, superconducting films.

I. INTRODUCTION

THE INTEREST in the analysis of texture formation in (Nb,Ti)N films is motivated by a need to develop a reliable production line for THz SIS mixers [1]–[3]. Many researchers have observed strong dependence of texture and film roughness on growth conditions for this class of materials [3]–[9]. However, only a few manuscripts are dedicated to a detailed analysis of texture and/or roughness formation. In this manuscript we present a characterization of various factors contributing to texture and surface morphology formation in our films, and relate the results to existing models.

In general, there are two contradicting concepts, based on either a thermodynamic or a kinetic approach, which try to explain the change in texture of the B1-type nitrides of transition metals [10].

Pelleg *et al.* propose a thermodynamic approach. They state that the degree of surface energy (S_{hkl}) is $S_{100} < S_{110} < S_{111}$,

while the degree of strain energy per unit volume, (u_{hkl}), is $u_{111} < u_{110} < u_{100}$. If one assumes that the surface energy does not depend on film thickness and that the strain energy increases with it, one can then determine the total of the surface energy and strain energy for a given plane (hkl). Due to the driving force to minimize the total energy, it would then be expected that [100] texture be preferred for relatively low film thickness, when the strain energy is less than the surface energy, with a change in texture with increasing film thickness to [110] and then to [111], because the strain energy starts to play a more dominant role in the determination of the total energy [11].

In contrast, Greene *et al.* state that a change in texture can be determined by kinetic effects such as incident particle distributions, nitrogen overpressure, orientation-dependent surface adatom mobility, etc. [12]. In particular they have shown that the presence of strain and/or changes in the state of strain throughout the film thickness are not requirements for obtaining changes in preferred orientation. We have proposed in our previous work, that adatom energy may be a key parameter of film growth in the case of magnetron sputtering at ambient substrate temperature [13]. Petrov *et al.* associate the change in rf-bias-sputtered TiN film texture with ion channeling [14]. They explain the change from [111] to [100] texture with an increase in ion assistance by the fact that the planes corresponding to easy ion-channeling and lower sputtering yields have the highest probability to survive. Since the processes of competitive grain growth determines the texture formation in these materials [12], an approach based on a ratio of growth rates of different facets is valid for this system as well [10]. For a cubic lattice, an increase in the ratio of {100} and {111} facet growth rates results in a transition of texture from [100] to [110], and finally to [111]. (It is interesting to note that, the texture evolution in this case is the same as in the thermodynamic model.) A transition from [111] to [110] texture occurs via the abundance of [11γ] textures, while a transition from [110] to [100] texture occurs via the abundance of [1γ0] textures, where $0 \leq \gamma \leq 1$. However, factors like crystallographic defects, a lack of surface diffusion, or an instrumental function of the growth apparatus, etc., may hamper the growth of particular facets. In this case the crystal habit and film texture may differ from the one expected from the ratio of {111} and {100} facet growth [10].

The surface roughness of these materials has received less thorough investigation. However, a number of experimental and theoretical reports are dedicated to the influence of technological factors like substrate bias, film thickness, nitrogen pressure, etc. [7], [9], [10].

IEEE TRANSACTIONS ON APPLIED SUPERCONDUCTIVITY, VOL. 13, NO. 2, JUNE 2003

II. EXPERIMENTAL

Films of (Nb,Ti)N are deposited by reactive magnetron sputtering in a Nordiko-2000 sputtering system with a base pressure of 4×10^{-5} Pa. In order to avoid the hysteretic sputtering regime, the pumping rate is fixed at a high value of 750 l/s for all experiments. Because the nitrogen injection is more than ten times lower than the argon injection in all experiments, the target material is sputtered mainly by argon atoms. A 99.8% pure alloy target with 30 at.% Ti and 70 at.% Nb is used. All films are sputtered by 300 W DC power and have a thickness of 480 ± 20 nm. Wafers are fixed to the copper chuck (maintained at 20 °C) with diffusion pump oil to stabilize the substrate temperature. A detailed description of the home-made 3 inch circular sputtering source used for film deposition is published in [13]. Ion assistance produced by this sputtering source has a very moderate influence on the film properties when compared with the changes caused by variations in sputtering pressure [13]. Gas densities are measured by inserting a small sampling pipe (attached to an external pressure gauge) between the sputtering source and the substrate. The details of this technique are discussed in the work of Rossnagel [15].

Films are deposited on 2 inch oxidized Si wafers. The stress in the films is evaluated by measuring the deflection of the wafer before and after film deposition with a profilometer. The transition temperature (T_c) is evaluated from the dependence of film resistivity on temperature. Film chemical composition is measured by Rutherford Back Scattering spectroscopy (RBS). Phase identification and texture measurements are performed with a Bruker-AXS D5005 diffractometer. Further details of RBS, XRD, and TEM analysis are published elsewhere [5]. Atomic force microscope (AFM) Nanoscope III (MMAFM-1) manufactured by Digital Instruments is used for film roughness characterization.

III. FILM PROPERTIES VS. SPUTTERING PRESSURE

We have optimized the nitrogen injection for a wide range of total sputtering pressures in order to obtain maximum T_c of the (Nb,Ti)N films. The limits of the pressure range are determined by film degradation caused by destructive bombardment of the growing film by fast neutrals at low pressures, and high thermalization conditions at high pressures [4]. Figs. 1 and 2 contain two sets of data for films deposited at the minimum substrate-target distance (4 cm) and the maximum substrate-target distance (8 cm). The deposition rates are 180 ± 10 nm/min and 80 ± 5 nm/min respectively. XRD analysis shows that all of the films have B1 crystal structure. Both sets of data show similar behavior versus sputtering pressure. T_c is seen to have a moderate dependence on the sputtering conditions, illustrating the well-known insensitivity of this value to structural defects in the B1 superconductors (Fig. 1). Compressive stress also shows a typical behavior versus sputtering pressure for magnetron sputtering systems: it decreases with increasing sputtering pressure (Fig. 1). The variation of the intensity ratio of the {200} and {111} XRD lines indicates substantial changes in the film structure (Fig. 1). Film roughness decreases with decreasing sputtering pressure for both substrate-target distances (Fig. 2). AFM scans of the samples marked on the Fig. 1 with the letters "a,"
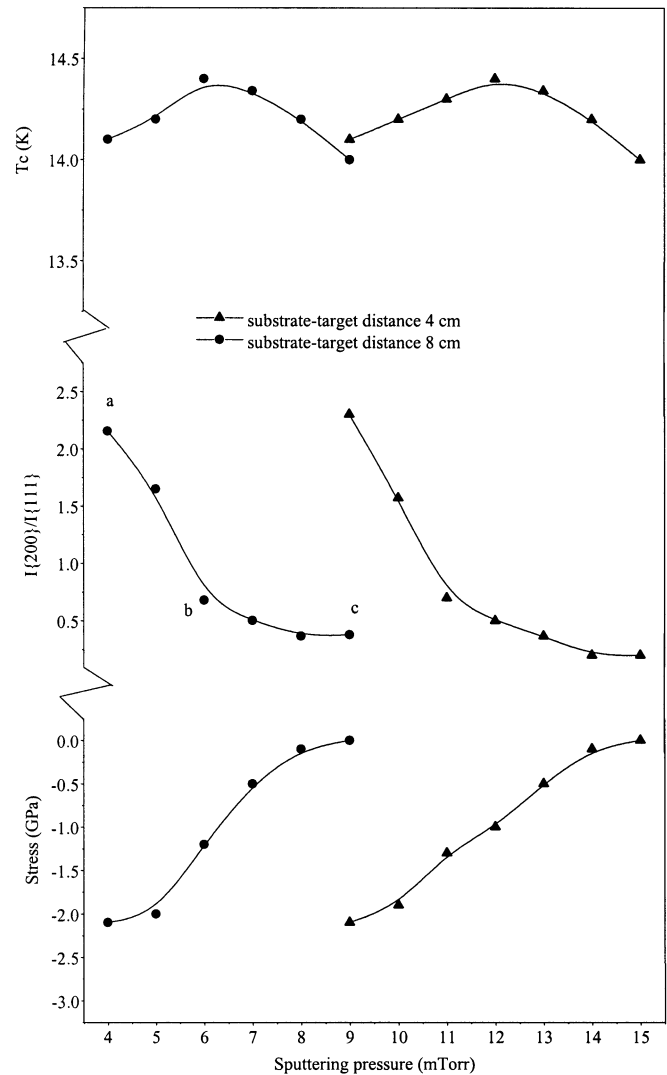

Fig. 1. T_c, ratio of [200] and [111] XRD line intensities, and intrinsic stress of (Nb,Ti)N films deposited at different substrate-target distance.

"b," and "c" are illustrated on the Fig. 3. Gas rarefaction becomes less pronounced at low pressures, since the hot particles of the sputtering yield have fewer collisions with the cold gas particles than at high pressures (Fig. 2). Gas cooling during sputtering is more effective at the minimum substrate-target distance, due to an instrumental function of the sputtering system. For this reason, gas rarefaction is stronger at the maximum substrate-target distance. RBS indicates that all films have almost stoichiometric compositions: a ratio of metal-nonmetal concentration of 1 ± 0.03, and a ratio of Nb and Ti in the deposited films that is the same as in the target.

IV. FILM PROPERTIES VERSUS NITROGEN INJECTION

In this experiment, the nitrogen injection is varied, while keeping the total sputtering pressure at 6 mTorr. The substrate-target distance is set to the maximum distance, and the limits of nitrogen injection are determined by the requirement to produce a B1-type crystal structure. The resulting deposition conditions and film properties are illustrated in Fig. 4. T_c is seen to have a moderate dependence on nitrogen injection, as
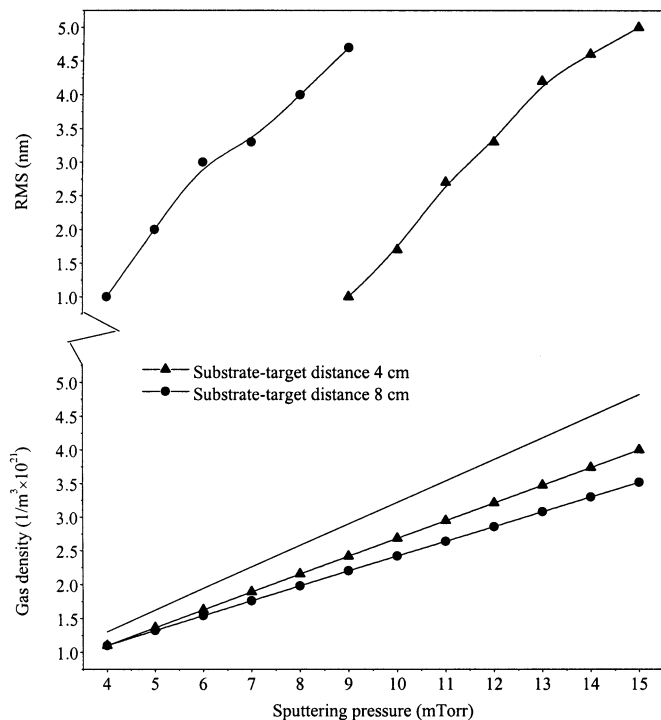
Fig. 2.   Film roughness and gas density between the substrate and the target for different substrate-target distances and sputtering pressures. A straight line on the bottom plot illustrates the gas density with no glow discharge.

in the first experiment. Compressive stress has a very moderate increase with nitrogen injection. This is presumably due to the fact that the fluxes of ions and fast neutrals bombarding the substrate surface are nearly independent of nitrogen injection, so that a reduction in deposition rate results in an increase in the effective intensity of the fluxes responsible for Ar peening. The deposition rate decreases with an increase in nitrogen injection, as is expected in reactive sputtering. The ratio of the {200} and {111} XRD peak intensities strongly decreases with increasing nitrogen injection. This is a clear indication that substantial changes in film texture also take place in this experiment. Despite the fact that the deposition rate decreases with an increase in nitrogen injection, gas rarefaction does not change. This is a clear indication that the particles of the sputtering yield become more energetic with an increase in nitrogen injection, causing the same gas rarefaction despite a reduction in numbers. Rossnagel reports similar results [15]. He shows that the degree of gas rarefaction caused by the flux of hot sputtered particles depends mainly on applied power and that the target material has almost no influence on this phenomenon. Increasing the nitrogen injection by a factor of two results in only a moderate increase in the nitrogen concentration in the films, indicating that we are operating in the region where the target surface is coated with nitride, and changes in nitrogen injection result primarily in a different depth of target nitridation [16].

V. ANALYSIS

The detailed XRD investigation of the texture revealed that in both of the experiments an increase of the ratio of {200}
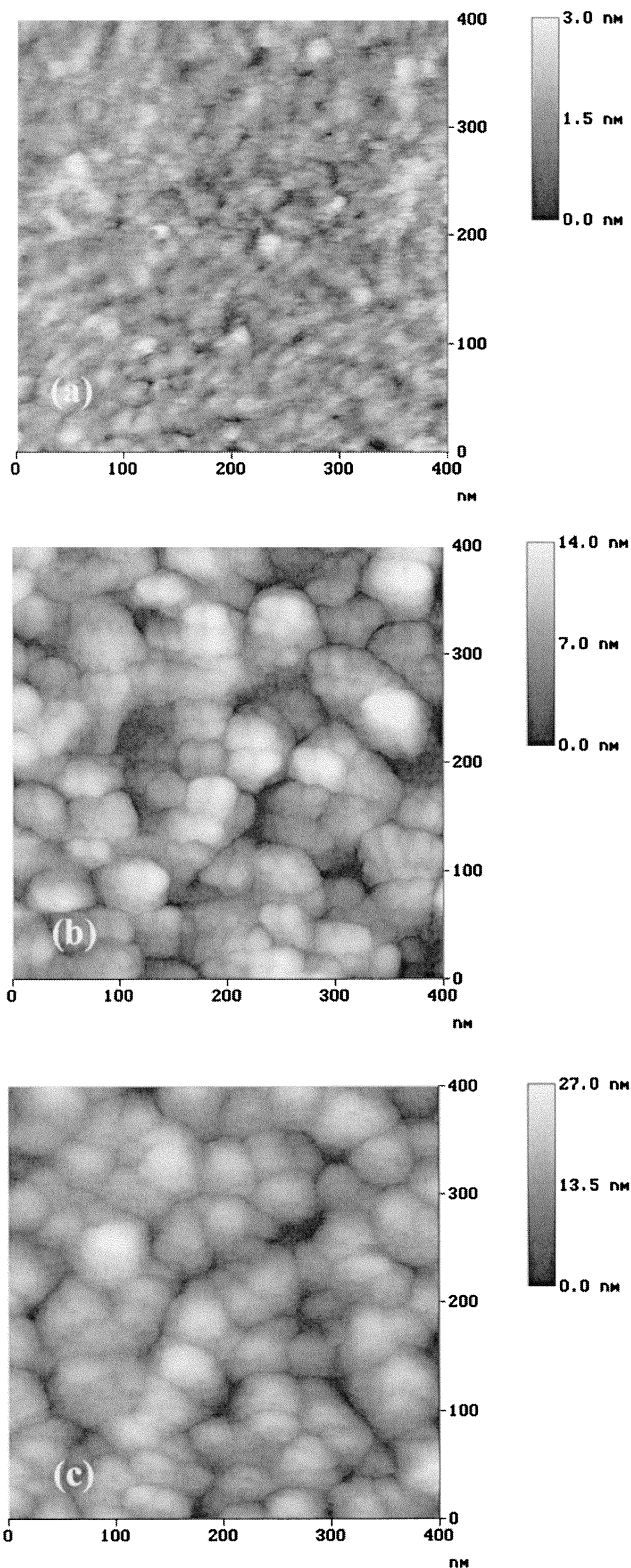

Fig. 3.   AFM scans of the samples sputtered under 4, 6, and 9 mTorr and 8 cm substrate-target distance [images (a), (b), and (c) correspondingly].

and {111} XRD peaks corresponds to a transition from [111] to [100] texture [5]. It is interesting to note that, in contrast with the case of texture determined by competitive growth, mentioned in the introduction, the change from [111] to [100] texture goes via the abundance of [1$\gamma\gamma$] textures, where $0 \leq \gamma \leq 1$. In other
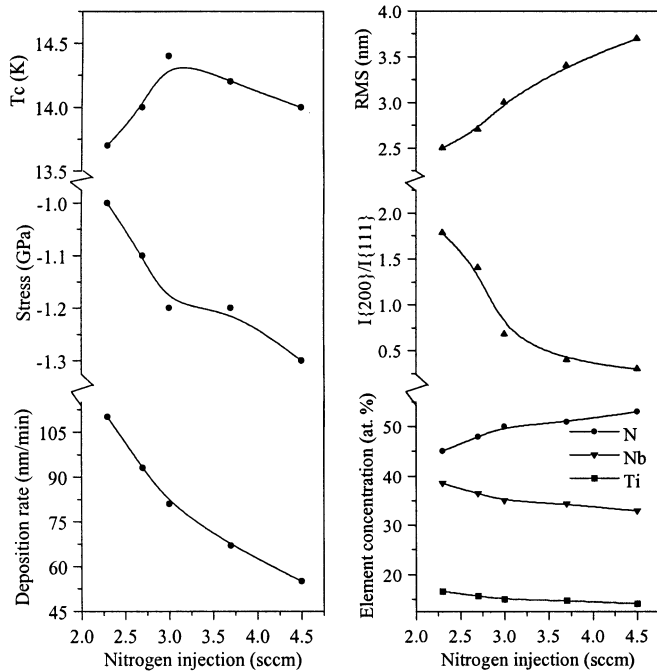
Fig. 4. T_c, film stress, deposition rate, surface roughness, ratio of [200] and [111] XRD line intensities, and chemical composition of the films deposited under different nitrogen injection.

words, the system makes a "short cut" bypassing [110] texture [5].

As seen from Figs. 1 and 4, an increase in compressive stress correlates with a change from [111] to [100] texture. Thus, the thermodynamic model does not describe our case, since it predicts the opposite behavior. As has been reported previously, ion assistance is quite weak and has a very moderate impact on film properties [13]. This allows us to exclude the ion-channeling approach as well. As seen from Fig. 1, the properties of films sputtered at minimum substrate-target distance are almost equivalent to the properties of films sputtered at maximum substrate-target distance and twice lower gas concentration. This is a clear indication that thermalization of the sputtering yield is a determining factor, i.e., the energy of the adatom is the factor that determines the process of texture formation. Increasing the adatom energy causes a change in texture from [111] to [100] in the experiment with pressure variation. This experiment also indicates, that there is no dependence of film properties on deposition rate, i.e., the surface diffusion is not suppressed by increasing the adatom arrival rate. However, as was mentioned previously, the adatom energy increases as the nitrogen injection increases, but the system is driven toward [111] texture. In other words, the film chemical composition has a very strong impact on texture development, overriding the effect of adatom energy.

Film roughness is in excellent correlation with the film texture when compared with other parameters, indicating that it is determined by crystal habit. Furthermore, film roughness plays a very important role when these films are used for junction production. The same thickness of AlN tunnel barrier used in SIS junctions with the bottom electrodes sputtered under the same conditions as films "a," "b," and "c" results in open circuit, critical current density of 1 kA/cm^2, and short circuit, respectively.

REFERENCES

[1] B. Bumble, H. G. LeDuc, J. A. Stern, and K. G. Megerian, "Fabrication of Nb/AlN$_x$/NbTiN junctions for SIS mixer applications," *IEEE Trans. Appl. Supercond.*, vol. 11, pp. 76–79, March 2001.
[2] Y. Uzawa, Z. Wang, and A. Kawakami, "Terahertz NbN/AlN/NbN mixers with Al/SiO/NbN microstrip tuning circuits," *Appl. Phys. Lett.*, vol. 73, pp. 680–682, March 1998.
[3] N. N. Iosad, V. V. Roddatis, S. N. Polyakov, A. V. Varlashkin, B. D. Jackson, P. N. Dmitriev, J. R. Gao, and T. M. Klapwijk, "Superconducting transition metal nitride films for THz SIS mixers," *IEEE Trans. Appl. Supercond.*, vol. 11, pp. 76–79, March 2001.
[4] N. N. Iosad, A. V. Mijiritskii, V. V. Roddatis, N. M. van der Pers, B. D. Jackson, J. R. Gao, S. N. Polyakov, P. N. Dmitriev, and T. M. Klapwijk, "Properties of (Nb$_{0.35}$,Ti$_{0.15}$)$_{1-x}$N$_x$ thin films deposited on silicon wafers at ambient substrate temperature," *J. Appl. Phys.*, vol. 88, pp. 5756–5759, November 2000.
[5] N. N. Iosad, N. M. van der Pers, S. Grachev, V. V. Roddatis, B. D. Jackson, S. N. Polyakov, P. N. Dmitiev, and T. M. Klapwijk, "Texture formation in sputter-deposited (Nb$_{0.7}$,Ti$_{0.3}$)N thin films," *J. Appl. Phys.*, to be published.
[6] N. N. Iosad, V. V. Roddatis, S. N. Polyakov, A. V. Varlashkin, B. D. Jackson, P. N. Dmitriev, and T. M. Klapwijk, "Superconducting transition metal nitride films for THz SIS mixers," *IEEE Transactions on Applied Superconductivity*, vol. 11, pp. 3832–3835, March 2001.
[7] J. M. Murduck, J. DiMond, C. Dang, and H. Chan, "Niobium nitride Josephson process development," *IEEE Transactions on Applied Superconductivity*, vol. 3, pp. 2211–2214, March 1993.
[8] J. Geng, A. Schuler, and P. Oelhafen, "Changing TiN film morphology by 'plasma biasing,'," *J. Appl. Phys.*, vol. 86, pp. 3460–3462, September 1999.
[9] R. Messier and J. E. Yehoda, "Geometry of thin film morphology," *J. Appl. Phys.*, vol. 58, pp. 3739–3746, November 1985.
[10] C. V. Thompson, "Structure evolution during processing of polycrystalline films," *Annu. Rev. Mater. Sci.*, vol. 30, pp. 159–188, March 2000.
[11] J. Pelleg, L. Z. Zevin, S. Lungo, and N. Groitoru, "Reactive-sputter-deposited TiN films on glass substrates," *Thin Solid Films*, vol. 197, pp. 117–128, March 1991.
[12] J. E. Greene, J.-E. Sundgren, L. Hultman, I. Petrov, and D. B. Dergstrom, "Development of preferred orientation in polycrystalline TiN layers grown by ultrahigh vacuum reactive magnetron sputtering," *Appl. Phys. Lett.*, vol. 67, pp. 2928–2930, November 1995.
[13] N. N. Iosad, B. D. Jackson, S. N. Polyakov, P. N. Dmitriev, and T. M. Klapwijk, "Reactive magnetron sputter-deposition of NbN and (Nb,Ti)N films related to sputtering source characterization and optimization," *J. Vac. Sci. Technol.*, vol. A19, pp. 1840–1845, July/August 2001.
[14] I. Pertov, L. Hultman, J.-E. Sundgren, and J. E. Greene, "Polycrystalline TiN films deposited by reactive bias magnetron sputtering: Effects of ion bombardment on resputtering rates, film composition, and microstructure," *J. Vac. Sci. Technol.*, vol. A10, pp. 265–272, March/April 1992.
[15] S. M. Rossnagel, "Gas density reduction effects in magnetrons," *J. Vac. Sci. Technol.*, vol. A6, pp. 19–24, January/February 1988.
[16] L. B. Jonsson, T. Nyberg, and S. Berg, "Target compound layer formation during reactive sputtering," *J. Vac. Sci. Technol.*, vol. A17, pp. 1827–1831, July/August 1999.